Article accepted for publication
in the Journal of the American Ceramic Society
(ISSN: 0002-7820, ESSN: 1551-2916).
October 2018.

Reduction of internal friction in silica glass with high OH content.

B.S. Lunin[1], K.V. Tokmakov[2,3]

The aim of this article is to investigate processes occurring during annealing of silica glass classified as being of type III [1]. This is an inexpensive silica glass produced by many manufacturers across the globe. However, it can be successfully used for fabrication of high-*Q* mechanical resonators. The relationship between residual internal stress and internal friction is elucidated. Quantitative analysis of the structural relaxation kinetics is presented. The influence of the cooling process for structural transformation is also discussed. Based on our results, we suggest optimal annealing conditions for minimizing internal friction type III silica glass. The results will be useful for further improvement of the Q-factor of mechanical resonators, including the test masses of the next generation of gravitational wave detectors. Our approach might, in addition, be used for studying the modification of atomic structure in multicomponent glasses.

Keywords: silica glass, internal friction, annealing, stress.

1. M.V. Lomonosov Moscow State University, Department of Chemistry. 119991 Moscow, Russia.
2. University of Glasgow, School of Physics and Astronomy. G12 8QQ, Glasgow, Scotland, UK.
3. At present: Aston University, School of Engineering and Applied Science, B4 7ET, Birmingham, UK.

1. Introduction

Silica glass is a well-known material used in instrument engineering and experimental physics for the fabrication of mechanical resonators with small dissipation. High-purity glasses such as Suprasil® 300 and 3001 (and others with impurity levels < 1 ppm) are the most common and well-proven choice of material in these applications. A wide range of mechanical resonators utilize the

unique low level of mechanical loss in silica glass, including hemispherical resonator gyroscopes (with a mass of a few grams) [1–4] and the test masses of modern gravitational-wave detectors (with mass = 40kg each) [5–7]. Note that the cost of high-purity glass is great due to the relatively complex manufacturing technology. At the same time, less expensive silica glass is also often characterized by low intrinsic mechanical loss (often called 'internal friction '). Widely-used type III silica glass, which is produced by a pyrolysis reaction of $SiCl_4$ in a hydrogen-oxygen flame [8,9], is an example of such low intrinsic loss material. The level of impurities in this glass is also very low, except for OH groups which can have a concentration as high as 1000-1300 ppm. This technique for fabricating silica glass was invented in the 1930s by J.F. Hyde from the “Corning Glass Works” and described in the US patent 2,272,342 [10,11]. Currently, many silica-glass manufacturers fabricate this type of silica glass under different trademarks: Suprasil-1 (Germany), Corning-7940 (USA), Tetrasil (France), 4040 (Japan), and KU-1 (Russia). The technology of silica deposition is relatively simple, so that the cost of such types of glass is smaller than the high-purity trademarks mentioned above.

Our early research proved that the level of intrinsic loss in type III silica glass can be very low, despite the high content of hydroxyl (OH) groups [12]. However, the intrinsic loss shows a strong dependence on the inner stresses of siloxane bonds (Si-O-Si). This type of glass can have significant internal stress, as it is usually produced in the form of large pieces at a high temperature. The cooling of these pieces leads to the appearance of significant thermal stresses, followed by the formation of structural defects; these defects affect the level of intrinsic stress. The *Q*-factor of resonators (equal to the reciprocal of the loss) fabricated from type III silica glass is relatively small, but it can be noticeably increased by annealing. For many materials a dependence of the internal friction on internal mechanical stress was observed. In this work we study changes in the glass structure during annealing and link those changes to differences in measured mechanical loss. Our results suggest ways to optimize the annealing process with a view to reducing internal friction.

2. Experimental methods.

Mechanical loss measurement and stress characterization

The experimental results presented in this article were obtained at Moscow State University over a period of more than two decades. We have selected some of these results that help to outline the patterns of physical processes responsible for changes in mechanical losses and support the discussion presented below in section 7. The experimental investigation was mainly focused on silica glass KU-1 (type III). For comparison, we also studied a few samples of high-purity glasses of type IV: a Russian brand KS4V [13] and Suprasil-300. The OH concentration of such glasses, as reported by their manufacturers, does not exceed 1300 ppm for KU-1, 0.1 ppm for KS4V[13] and 1 ppm for Suprasil-300[14]. We measured the intrinsic losses by observing the free decay of eigenmodes in both stressed and annealed silica-glass cylinders (figure 1a). The temperature and duration of annealing were chosen based on the results of a subsidiary spectroscopic experiment, using samples made from the same brand of silica glass. In addition to the reduction of stress, which reduces mechanical loss, annealing might lead to cracking of the glass surface. This latter effect increases mechanical loss and is discussed in section 6.

The direct measurement of internal stress can be complex. However, the speed of sound in silica directly depends on the internal stress, and can be easily measured. Here, we used a special setup[12] to measure both the speed of sound and the intrinsic loss (figure 1b). The test resonators were manufactured in the shape of cylinders (1) with length L lying in the range 80-120mm and diameter D from 15 to 80mm. All surfaces were polished and chemically etched to minimize additional loss arising in a near-surface layer. The final surface cleaning was performed in baths containing sulphuric acid and hydrogen peroxide solutions. The glass cylinders were tested in a vacuum tank allowing *in situ* heating (2). The cylinders were suspended in equilibrium on a

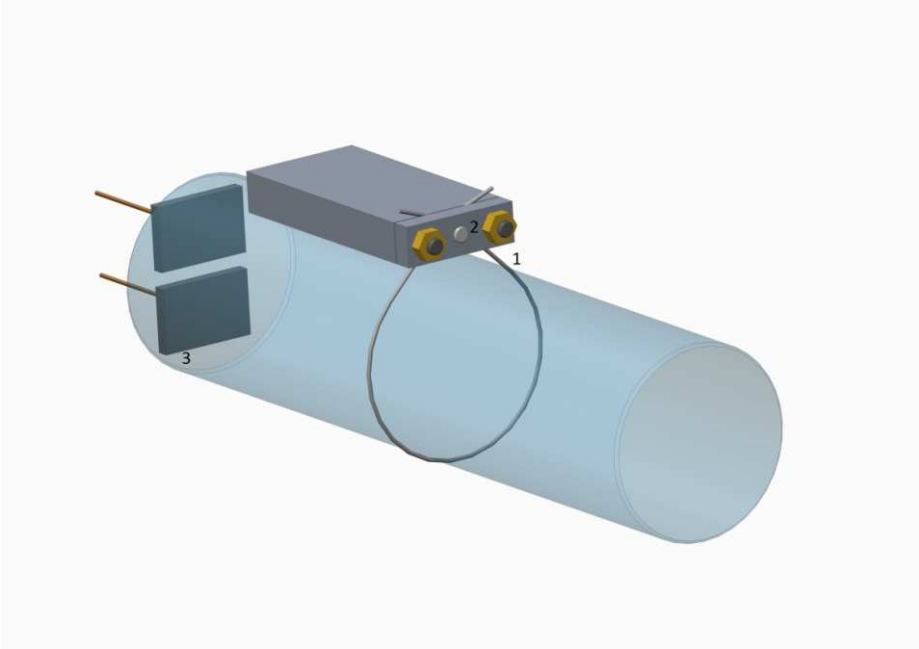

Figure 1a. Schematic of a silica cylinder suspended for measurements of the free amplitude decay. A polished 50 μm diameter tungsten wire (1) forms a loop in the plane of the node of longitudinal oscillations. The wire is crossed below the clamping plate. The pin (2) for holding the wire simplifies the process of cylinder installation. The readout electrodes (3) are shown behind the back face of the cylinder. Similar electrodes for excitation installed near the front of the cylinder (item 5 in fig. 1 b) are omitted on this picture.

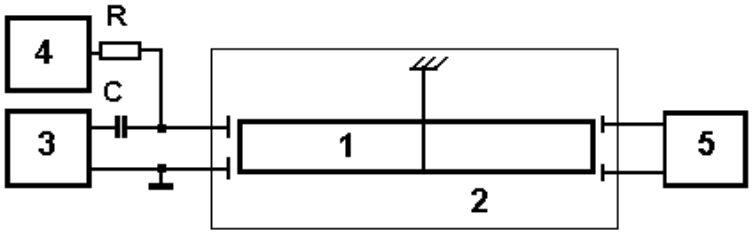

Figure 1b. Schematic of the experimental setup for measuring intrinsic mechanical losses (the free decay oscillation) and the speed of sound in the silica-glass cylinders. 1-silica cylinder; 2-vacuum tank allowing *in situ* heating; 3-AC generator; 4-DC power supply; 5-capacitive displacement sensor assembly.

50μm tungsten wire as shown in figure 1a. Capacitive displacement sensors and excitation actuators were installed near the faces of the cylinder. To excite longitudinal mechanical oscillations, we applied an AC voltage at the resonant frequency f and a bias (a DC offset) to the actuators. The amplitude of the AC voltage (supplied from the signal generator 3) was 300-500V, while the DC bias produced by the power supply 4 was in the range from 500V to 1000V. The operation of the readout sensor was based on changing the capacitance of a planar electrode (see fig. 1) integrated into a radiofrequency oscillator. Low frequency variation of its capacitance caused by the displacement of the cylinder face led to modulation of the high frequency pump signal. The low frequency component, proportional to the longitudinal oscillation of the cylinder, was extracted by a low-pass filter and used for subsequent analysis.

The speed of sound V_{sound} was calculated from the longitudinal resonance frequency and the sample length using the formula $V_{sound} = 2Lf$.

The same setup was used for measuring the mechanical loss of the silica test samples. The mechanical loss (ξ) is the inverse of the Q-factor: $\xi = Q^{-1}$. The Q was found from the exponential time constant, τ^*, for the free decay of the longitudinal eigenmodes: $Q = \pi f \tau^*$. The uncertainty provided by this method of measurement was near 2-3%. The reproducibility of measurements was good, but nevertheless we usually took a series of measurements and chose those with the largest Q. This is a common approach to distinguish losses in the resonator from inconsistent losses in the suspension[15,16].

The IR absorption spectra reported in section 4.2 were measured on the Fourier spectrometer Equinox 55/S (“Bruker”).

3. Experimental results

3.1. Measurement of mechanical losses.

Figure 2 shows our measurements of the mechanical *Q*-factor of samples of type III and type IV silica glass. Some of the samples were annealed while others were measured in the state in which they were received from the manufacturer. These measurements illustrate the obvious statement that the level of internal losses cannot solely be attributed to one factor (such as the absolute purity of the glass). Note that annealing of the KU-1 sample at a temperature of 900°C produced a higher *Q*-factor than annealing at 980°C.This result is not obvious and requires analysis of all factors that influence the experimental data. First it should be noted that differences in the measured Q cannot be attributed to variations in the losses associated with the suspension of test samples. To estimate the contribution of the suspension to the total loss, a similar sized cylinder fabricated from a sapphire monocrystal was suspended on the same tungsten wire. A $Q \gtrsim 1.6 \times 10^8$ was measured at room temperature: this was significantly lower than values reported in the literature[17,18], which are close to 3×10^8. The difference of the inverse Q-factors $\Delta Q^{-1} \approx 2.9 \times 10^{-9}$ can be considered as a rough estimate of the suspension contribution to the total loss. This contribution creates a systematic bias in the measured data. The changes of measured losses after resuspension of the test sample should be far smaller than the systematic error. The loss increase between the silica glass samples annealed at 900°C and 980°C is already larger than this systematic error ($\Delta Q^{-1} \approx 8 \times 10^{-9}$ for room temperature and $\Delta Q^{-1} \approx 5 \times 10^{-9}$ for the peak values). Therefore, the difference in Q-factors cannot be explained by the statistical variation in the suspension losses. The observed physical effect of the annealing temperature on the level of internal stress, and eventually on the level of mechanical losses, will be studied in sections 4-6.

Here, we begin by investigating losses in highly-stressed silica glasses. Figure 3 shows the measured losses in non-annealed KU-1 glass. It is more convenient to present these as the dependence of internal friction Q^{-1} on inverse temperature T^{-1}. We fitted two peak functions

(represented by the dotted lines) to the experimental data. The sum of the fitted peaks is shown by a solid line. The wide dissipative peak with maximum located near $T^{-1} \approx 3.1\times10^{-3}\,K^{-1}$, i.e. T ≈ 50-60°C (for measurement frequency 30-40 kHz) can be attributed to the influence of internal stresses; arguments for this statement can be found in[19].

3.2. Characterization of the internal stress.

3.2.1. Mechanical losses in relation to the speed of sound: experimental study.

The level of internal stress can be linked to the speed of sound in silica glass (see further comments in 3.2.2); this relationship is of great practical use since the speed of sound V_{sound} can be obtained in a relatively simple experiment. Figure 4 shows the measured dependence of the *Q*-factor of silica cylinders on the speed of sound. These data were obtained at different stages of the annealing process (which is reviewed in greater detail below in section **4**). A linear fit to the experimental data is shown by the dotted line.

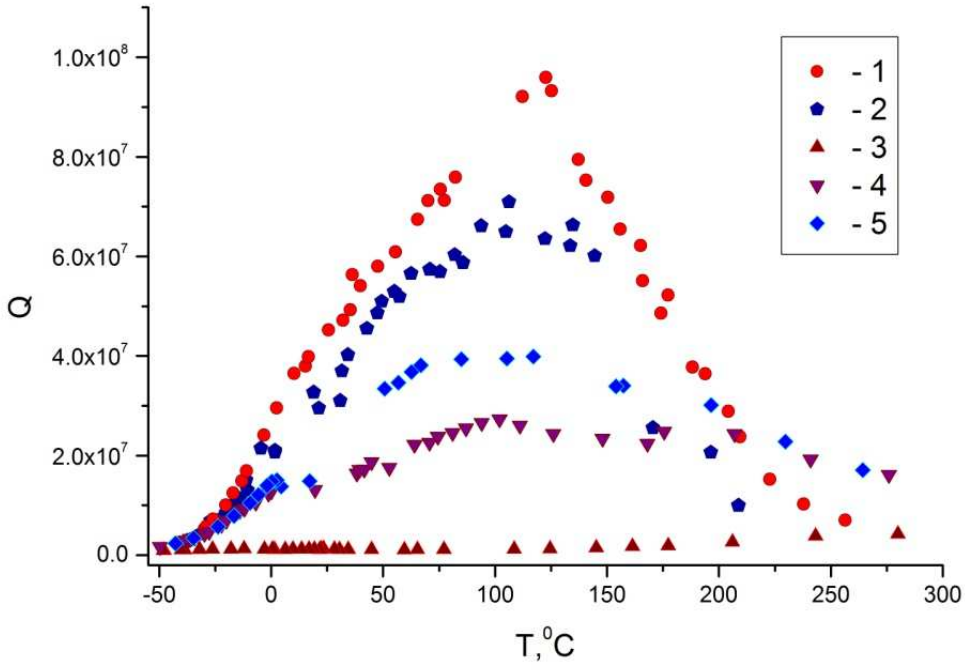

Figure 2. *Q*-factor measured in mechanical cylinders (fabricated from silica glass KU-1, KS4V and Suprasil-300) plotted against temperature. 1 – KU-1 annealed at 900°C; 2 – KU-1 annealed at 980°C; 3 – KU-1, not annealed; 4 – Suprasil-300, not annealed; 5 – KS4V, not annealed.

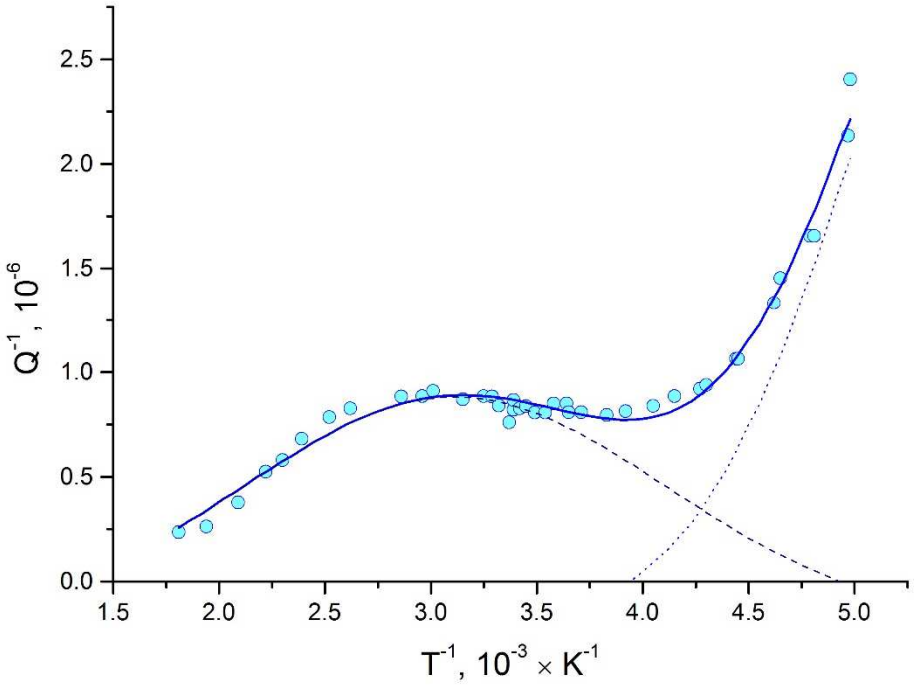

Figure 3: Internal friction vs inverse temperature in stressed silica glass KU-1.

The blue filled circles represent experimental results. The experimental data are fitted by two peaks (shown by the dotted and dashed lines); their sum is shown (solid line).

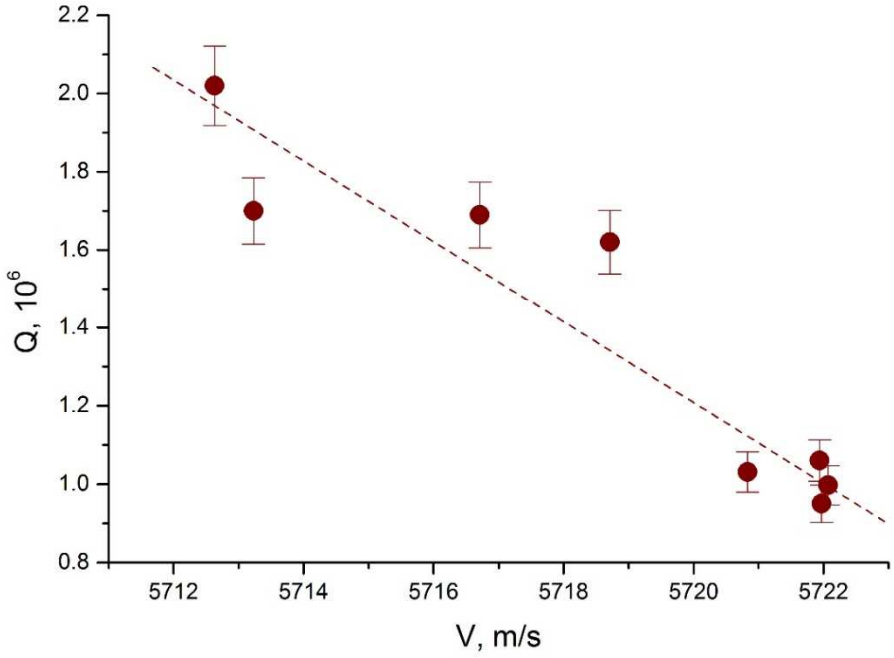

Figure 4. Dependence of the *Q*-factor of silica cylinders on the speed of sound. Experimental data are shown by the filled circles. A linear fit to the experimental data is shown by the dashed line.
The test samples (length and diameter $D \approx L \approx 80$ mm) were made from the glass KU-1.

3.2.2. Losses in relation to internal stress: calculation.

According to Strakna et al. [20], a change in the speed of sound V_{sound} of 10 m/s (see Figure 4) is equivalent to a change in internal stress by ~17 MPa (175 kg/cm^2). This agrees in order of magnitude with an estimate of stress in large silica pieces. Figure 4 shows that the mechanical *Q*-factor of silica glass is strongly correlated with the speed of sound and thus with internal stresses. Let us estimate the maximal allowed residual stress, of which the contribution to the total loss budget can be assessed as negligible. Assume that the *Q*-factor reduction in Figure 4 is entirely attributable to internal stress. In that case, the stress σ = 1 kg/cm^2 (9.8×10^4 Pa) leads to the appearance of internal friction $\xi = 2.9 \times 10^{-9}$. We can assume that a silica-glass resonator, free from internal stress, displays a *Q*-factor of 3×10^7, that is $\xi = 3.3 \times 10^{-8}$. Suppose that the internal stress may increase this value by a maximum of 1%, i.e., the loss contribution cannot be more than

$\Delta\xi \leq 3.3 \times 10^{-10}$. In this case, the residual internal stress should not be larger than σ_{max} = 11.8 kPa (≈ 0.12 kg/cm^2). We will refer to this target in our discussion of the reduction and increase in the internal stress after the annealing and cooling of the test sample (section 5).

4. Annealing of silica samples

4.1. Relaxation of glass structure during annealing. Theoretical preamble.

The heating of glass triggers a number of different physical process. The kinetic parameters of these processes depend on the atomic network structure, purity, and OH-content of the silica glass. Peculiarities of the type-III glass should be considered before choosing the temperature and duration of the annealing procedure.

Glass is often described as a liquid with extremely high viscosity. The key element of the atomic structure is a silicon-oxygen ring that can contain between three and eight silicon atoms and a corresponding number of oxygen atoms[21–24]. The ring structure of the atomic network is usually studied by means of Raman and Nuclear Magnetic Resonance spectroscopy[25–27]. Molecular dynamic simulations reported in the last two decades have improved our understanding of the relationship between the structure of glass and its mechanical properties, see for example[28–31]. The relative concentration of silicon-oxygen rings of different sizes depends on the details of the melting procedure. Cooling the glass melt down leads to the relaxation of the relative concentration towards a new equilibrium state. The number of highly-stressed rings (containing from three to four silicon atoms) tends to decrease while the relative concentration of the comparatively low-stressed rings (of five and more silicon atoms) increases[21,32]. Quick cooling of the glass melt increases the viscosity reducing the rate of structural relaxation. As a result, the glass solidifies in a stressed state and its structure remains far from a new equilibrium. The concentration of

structural rings can be returned to close to the equilibrium state by long annealing at a constant temperature.

Note that post-annealing cooling triggers a new relaxation process in which number of atoms in the Si-O rings tends to increase again. However, full rearrangement to a new equilibrium state requires a long time. The structural relaxation in samples with high OH concentration practically stops at some intermediate state at a temperature close to approximately 750^0C. The temperature reduction to this temperature is likely to be too fast to allow the closure of all Si-O rings in the new atomic structure. We can, therefore, expect that some of the atomic chains (broken rings) solidify in a state in which they are bent at non-standard angles. The temperature gradient that always appears during cooling aggravates stresses and provokes a rise of internal friction. In view of this, the parameters of the cooling process should be optimized.

4.2. Annealing of silica glass of type III. Supplementary experimental investigation.

The duration of annealing at the chosen temperature (directly dependent on the time of structural relaxation) is a parameter of high practical importance. To find the relaxation kinetic parameters in the temperature range 825-980^0C, we conducted an additional experiment with silica discs of 10 mm diameter and 1.7 mm thickness. We used a method based on an infrared (IR) spectroscopy technique suggested by Tomozawa et al. [33]. The peak, located around wavenumber 2260 cm^{-1} in the IR absorption spectrum, depends on the atomic structure of SiO_2 glass.

During annealing, the large rings separate into fragments, which form new, shorter rings. The concentration of the relatively large rings decreases while the concentration of short rings increases. This proportion approaches its equilibrium state at an exponential rate. As a result, the peak located near wavenumber 2260 cm^{-1} (measured between annealing cycles) also changes its position exponentially along the wavelength axis.

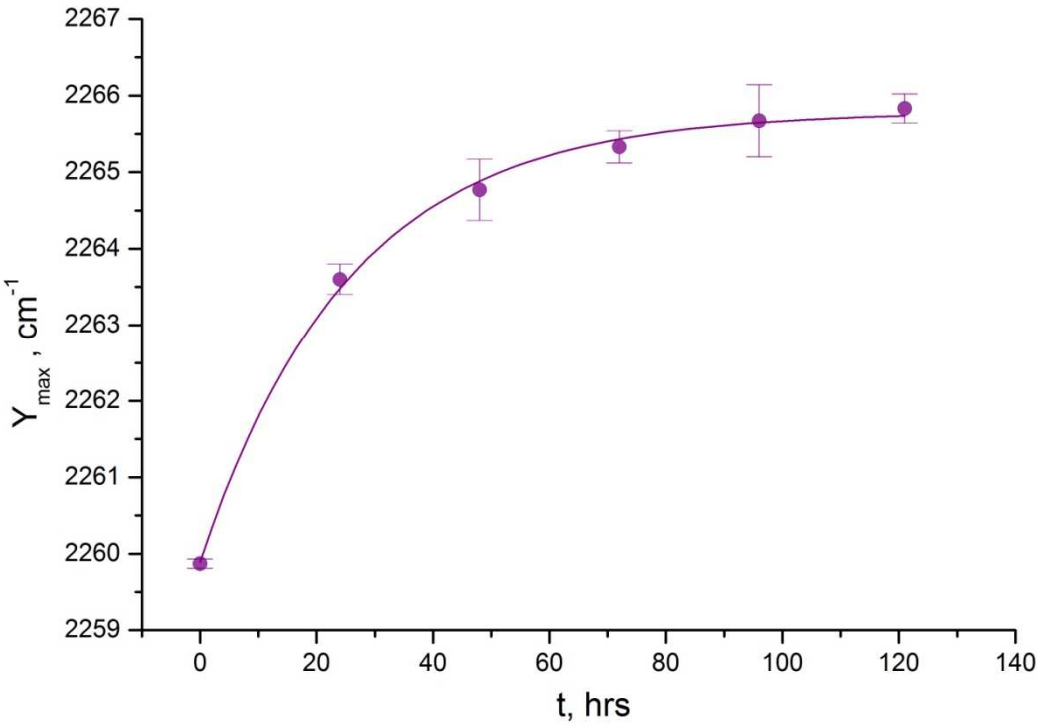

Figure 5. Alteration of the wavelength corresponding to the maximum of the peak in an IR absorption spectrum located near wavenumber 2260 cm^{-1} during annealing of a KU-1 silica-glass sample at temperature 890°C. Experimental data are shown by the filled circles. The exponential fit to the experimental data is shown by the solid line.

The IR absorption spectra were measured on a Fourier spectrometer EQUINOX 55/S ("Bruker"). The experimentally-obtained parameters of the relaxation of the IR peak position can be used as a characteristic of the structure modification during annealing [33].

An example of such exponential alteration is shown in Figure 5. A sample of KU-1 glass was annealed at 890°C in a silica ampoule in air. The sample was regularly taken out of the oven to measure the IR absorption spectrum. The total annealing time at a constant temperature is shown on the *x* axis, while the position of the maximum of the peak near 2260 cm^{-1} is shown on the *y*

axis. The experimental data were modeled with the function $Y_{\max} = \bar{Y}_{\max} - A\exp\left(-t/\tau\right)$. Fitting to this returned the time constant of the relaxation of the glass structure τ and the position of the peak maximum $\bar{Y}_{\max}$, which corresponded to the condition of structural equilibrium at the chosen annealing temperature. A similar experiment (and the subsequent model-fitting) was repeated for many values of temperature.

Figure 6 shows the dependence of $\bar{Y}_{\max}$ against the reciprocal of the annealing temperature. As elsewhere [33], these points were fitted by a linear function yielding $\bar{Y}_{\max} = 2234.78 + \frac{36159.59}{T}$ [cm^{-1}]. The similar linear dependence found before [33] is shown by the dotted line; see section 4.3 below. The previous experiment [33] was conducted in the temperature range 950-1400^{0}C, which only slightly overlaps with our temperature range 825-980^{0}C. The dotted line shown on the figure is extrapolated to cover our temperature range.

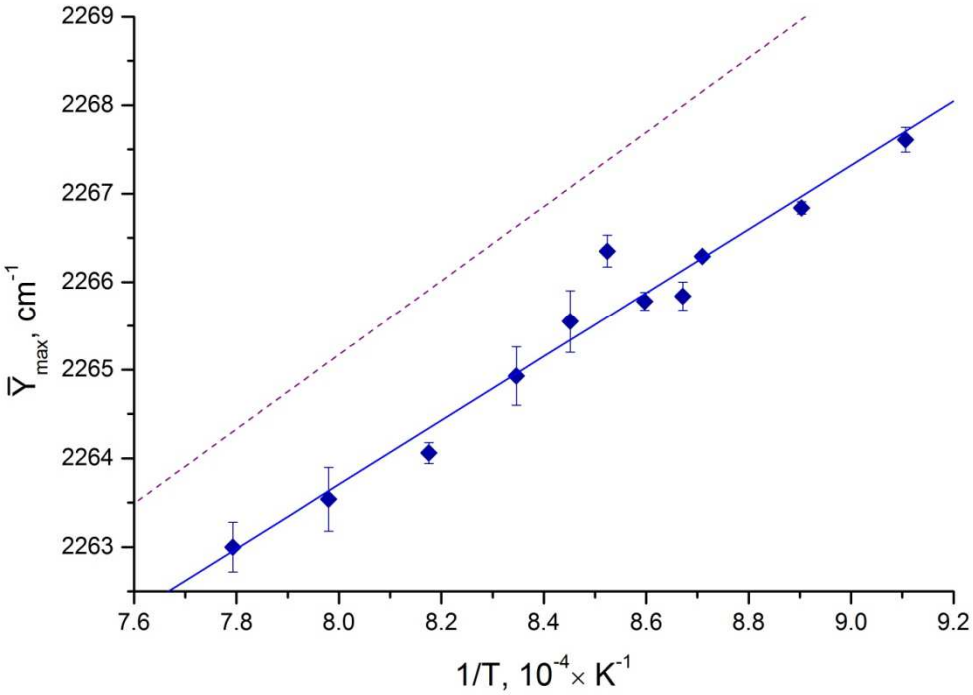

Figure 6. Dependence of the maximum of the peak in an IR absorption spectrum located near wavenumber 2260 cm^{-1} vs inverse temperature. The position of the peak $\bar{Y}_{\max}$ conforms to the fully

relaxed structure of the KU-1 silica glass after long annealing. The linear fit of the experimental data is shown by the solid line. The dashed line displays the similar dependence fitted to the data from [33] obtained for glass with a low concentration of OH groups.

Figure 7 demonstrates the dependence of the time constant of the relaxation of the glass structure τ to the annealing temperature. The data were fitted to the function $\tau = \tau_0 \exp\left(E/RT\right)$, where T is temperature and R is the molar gas constant. To find the activation energy E and the pre-exponential factor τ_0, we replotted the data as $\ln\tau$ against inverse temperature T^{-1} and fitted the data points with a linear function (not shown). We estimated the activation energy for the silica glass KU-1 to be ≈ 359 ± 27 kJ/mol. The estimated expression for the time constant of the relaxation of the glass structure for the silica glass KU-1 is

$\tau = 2 \times 10^{-15} \cdot exp[(3.59 \times 10^5)/RT]$ [hrs].

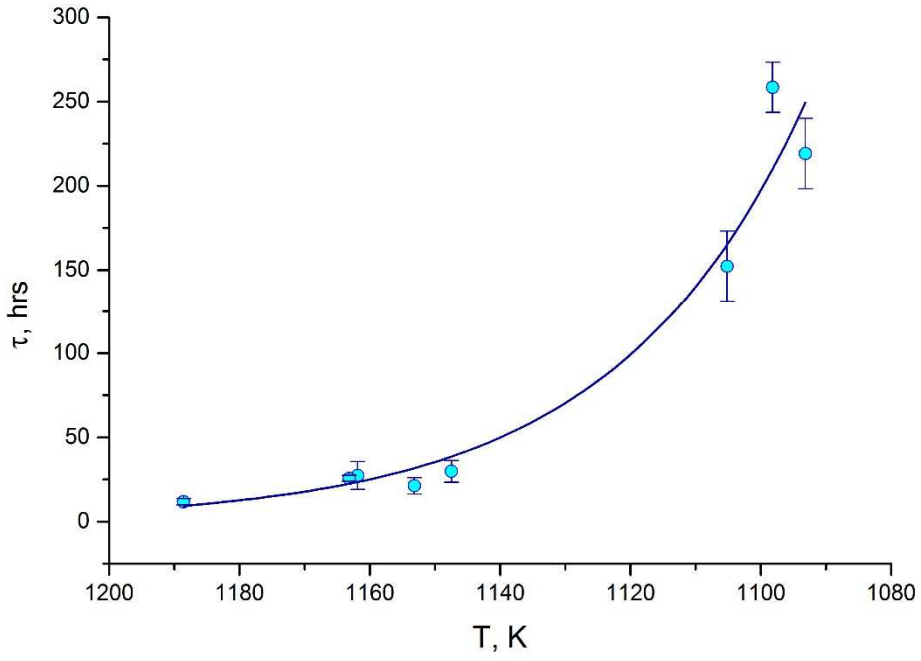

Figure 7. Time constant of the relaxation of the KU-1 glass structure against temperature of annealing.

4.3.Data review and practical recommendation.

Note that the dependence $\overline{Y}_{\max}(T^{-1})$ found in our experiment is different from a similar result reported elsewhere [33]: see Figure 6. We can attribute that to the lower strength of type III silica glass (due to the presence of hydroxyl groups) in comparison to the water-free glass IV studied in [33].

The temperature dependence of the structure relaxation time constant $\tau(T)$ allows the calculation of the duration of annealing for type III silica glass in the 825-980^{0}C temperature range. In our view, the quasi-equilibrium state can be achieved during a time equal to ~ 3τ. This time is presented in Table 1. Note that the temperature of glass transition T_g (taken as the temperature at which the viscosity is equal to 10^{12} Pa·s) for KU-1 is 1080°C [34].

Annealing temperature, ^{0}C	Duration of annealing, hours
800	1386
850	234
875	102
900	46
920	25
980	4.5

Table 1. Recommended duration of annealing of silica glass of type III

However, we shall demonstrate that a low annealing temperature leads to the formation of less-stressed ring structures, and, in that particular respect, is more beneficial.

A similar glass structure can be formed in OH-free glasses of type IV; however annealing at the same temperature needs to be of much longer duration due to the higher temperature of softening.

5. Appearance of stress during cooling

5.1. A new distortion from structural equilibrium

The state of structural equilibrium (achieved during isothermal annealing) is disturbed while cooling the glass sample down. The viscosity of the glass rises very quickly; as a result, all structural relaxation comes to a stop. However, non-isothermal cooling might significantly change the structure of the glass. Such cooling leads to the appearance of a temperature gradient directed perpendicular to the glass surface. For example, for a flat silica glass plate with thickness *h* cooling down with rate *v*, the temperature difference between the central plane and the surface, ΔT, is equal to [35]:

$$\Delta T = \frac{h^2 v C \rho}{8\chi}, \tag{4}$$

where ρ is the density ($2.21\times10^3 kg/m^3$), *C* is the specific heat (728 *J/kg·K*) and χ is thermal conductivity (1.38 *W/m·K*).

The resulting thermal stress is described by:

$$\sigma = \frac{2E\alpha\Delta T}{3(1-\upsilon)}, \tag{5}$$

where *E* is the Young's modulus (7.36×10^{10} Pa); α is the thermal coefficient of linear expansion ($6\times10^{-7}\ K^{-1}$) and υ is the Poisson ratio (0.18).

Distortion of the structure can be described by a kinetic equation of the first order. Here we assume that the parameter of structural relaxation obtained in the annealing spectroscopic experiment remains the same during the cooling of the silica glass:

$$\frac{\Delta c}{c_0} = 1 - exp\left[-\frac{1}{2\times10^{-15}}\int_0^{t_c} exp\left(-\frac{3.59\times10^5}{R(T_0 - vt)}\right)dt\right], \tag{6}$$

where c_0 is the concentration of non-distorted structural elements, Δc is the concentration of disturbed structural elements, T_0 is the temperature of the isothermal stage of annealing, v is the rate of temperature decrease, and t_c is the duration of the non-isothermal cooling stage. Internal friction arising from the distorted structural elements can be expected to be larger than the internal friction emanating from units in equilibrium. The stress also increases the level of internal friction. Therefore, as a first approximation, we can describe the structural distortion by the product $\sigma\Delta c/c_0$.

Let us estimate a few useful values. Consider the cooling of a cylinder with a diameter of 0.1 m. Let us assume that the formulae (4) and (5) derived for a flat plate can be used for the cylindrical test sample. The results of the calculation for the thermal stress of three different rates of cooling are shown in Table 2.

Rate of cooling v, ^{0}C/hour	ΔT, K	σ, Pa	σ, kg/cm^2
10	4.2	149700	1.5
5	2.1	74600	0.75
1	0.42	14970	0.15

Table 2. Thermal stress occurring during cooling of a silica glass cylinder of diameter 0.1 m

These values of thermal stress are not smaller (and sometimes significantly larger) than the acceptable limit $\sigma_{\max}$ calculated from the speed-of-sound experiment in section 3.2.2.

Let us examine the structural distortion $\Delta c/c_0$ under cooling with different rates and for different annealing temperatures T_0. Assume that any structural changes in the silica glass of type III stop at temperature 750^{0}C. Figure 8 presents the result of the numerical integration of expression (6).

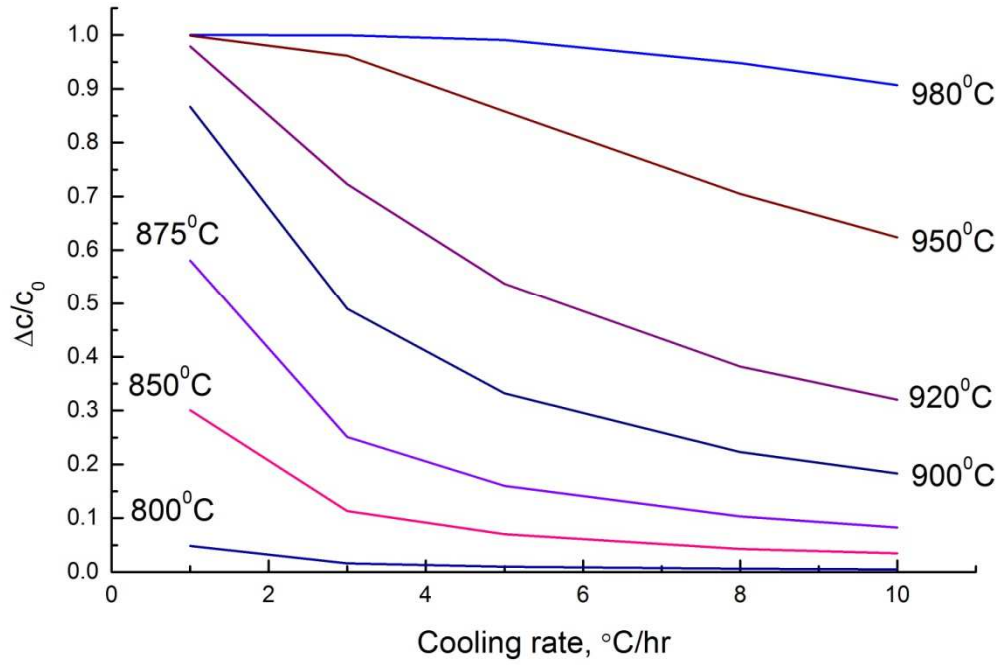

Figure 8. . Degree of distortion of the atomic structure in silica glass of type III (dimensionless value) against rate of cooling plotted for different temperatures of annealing.

The distortion of the atomic structure is larger if the annealing temperature is relatively high. The structure of the glass changes quickly enough to follow the temperature descent. Figure 9 shows the relation of the measure $\sigma\Delta c/c_0$ (calculated for a silica cylinder of diameter 0.1 m) depending on the cooling rate and the annealing temperature. The internal stresses are calculated from (4) and (5).

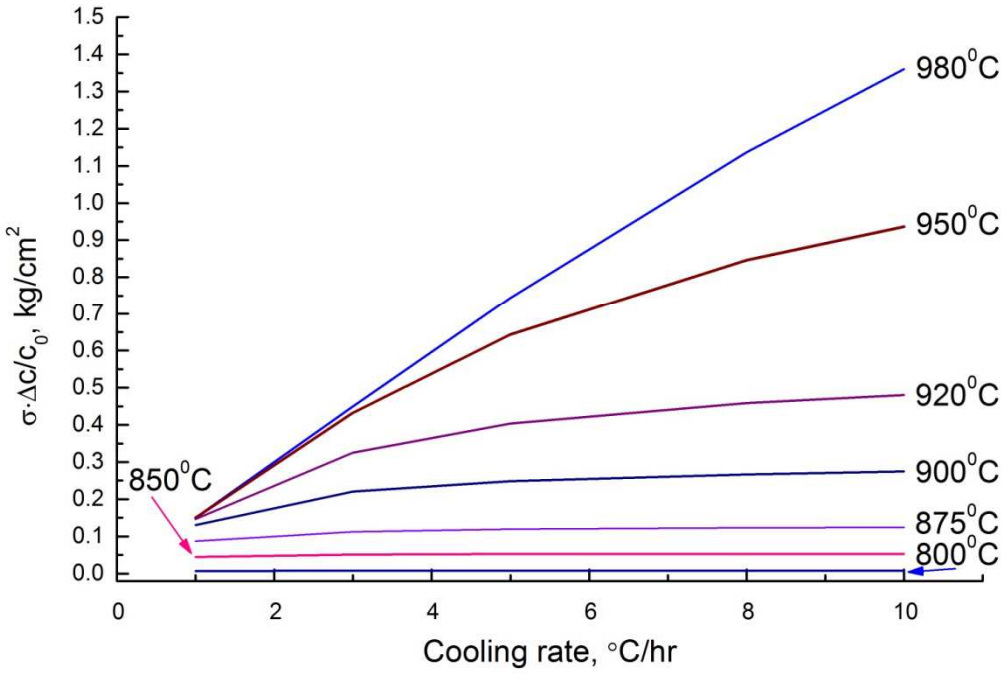

Figure 9. Distortion of the structure of silica glass presented in terms of the thermal stresses depending on the rate of cooling and the annealing temperature for the cylinder of diameter 0.1 m.

These figures reveal that the closest approach to the equilibrium state can be achieved by annealing at low temperatures (800-850^{0}C). The rate of cooling is not crucially important in this case and the structure of the glass is not significantly disturbed, even at dT/dt = 10 ^{0}C/hour. The same cooling rate chosen for glass annealed at T = 980°C would lead to the full distortion of the atomic structure of type III silica glass.

5.2.Mechanical losses in distorted solids

It is appropriate to discuss losses in silica glass samples at this point. First of all, we refer to the theory of inelastic relaxation in solids[36,37]. This phenomena is usually explained through schematic mechanical models, for example, the Voigt–Kelvin model[36,38]. The mass and spring oscillator in this model are complemented by a third element, a damper (a plunger), introducing delay in the reaction. The relationship between strain and stress in such a model is described by a modified Hooke's law containing the time derivatives of stress and strain. In the case of periodic

deformations, the stress in such a model is phase shifted with respect to the strain by a small angle. The solution of this oscillator equation is a periodic function with an exponentially-decaying amplitude. The Q-factor of the oscillator is determined by the phase shift between the stress and the strain. This simplified model illustrates an important idea: structural relaxation leads to the occurrence of energy loss. It is important that relaxation is not necessarily a rearrangement of an atomic structure. One of the main mechanisms of losses in fused silica is based on the effect of scattering of phonons on the acoustic vibrations of atomic chains[39]. The ensemble of phonons relaxes to its temperature equilibrium afterwards; this relaxation also leads to losses of mechanical energy. Unlike many other phonon-related effects (observable in experiments at cryogenic temperatures only), this phenomenon can be observed at room temperature.
Let us now return to the comparison of silica glass samples annealed at 900°C and 980°C. The atomic structure of silica glass annealed at 980°C contains more unclosed rings. The concentration of highly deformed rings (containing relatively few Si-O groups) is also larger. The frequency range of the vibrations of such chains is wider. For this reason, the activation energy of phonon scattering is higher and distributed across a wider frequency band in comparison to the structure formed after annealing at 900°C. In this way, phonon-phonon scattering in a more distorted glass structure results in larger energy dissipation. We believe that the distortion parameter plotted in Figure 9 can be used as a relative measure: to achieve a large Q-factor, the distortion parameter $\boldsymbol{\sigma \cdot \frac{\Delta c}{c_0}}$ should be minimized.

6. Surface dehydroxylation in type III silica glass triggered by annealing

As already mentioned, type III silica glass has a high content of hydroxyl groups. Prolonged heating (annealing) induces the dehydroxylation process in a sufficiently thick near-surface layer. Early work [40] reported experiments monitoring changes of OH concentrations during the annealing

of the silica glass KU-1. The diffusion coefficient of OH groups found using IR spectroscopy in [40] depends on temperature as $D = 8.83\times10^{-9}\exp(-15537/T)$, m^2/sec.

The relative concentration of OH groups at a depth H from the surface of a flat test sample of thickness h after annealing throughout time t_0 can be calculated using the formula [41]:

$$\frac{[OH]}{[OH]_0} = \frac{4}{\pi}\sum_{n=0}^{\infty}\frac{(-1)^n}{(2n+1)}e^{\frac{-D(2n+1)^2\pi^2 t_0}{h^2}}\cos\frac{\pi(2n+1)(h-2H)}{2h}. \qquad (7)$$

Such relative concentrations computed for four annealing regimes are plotted in Figure 10, which clearly shows the formation of a dehydroxylated layer.

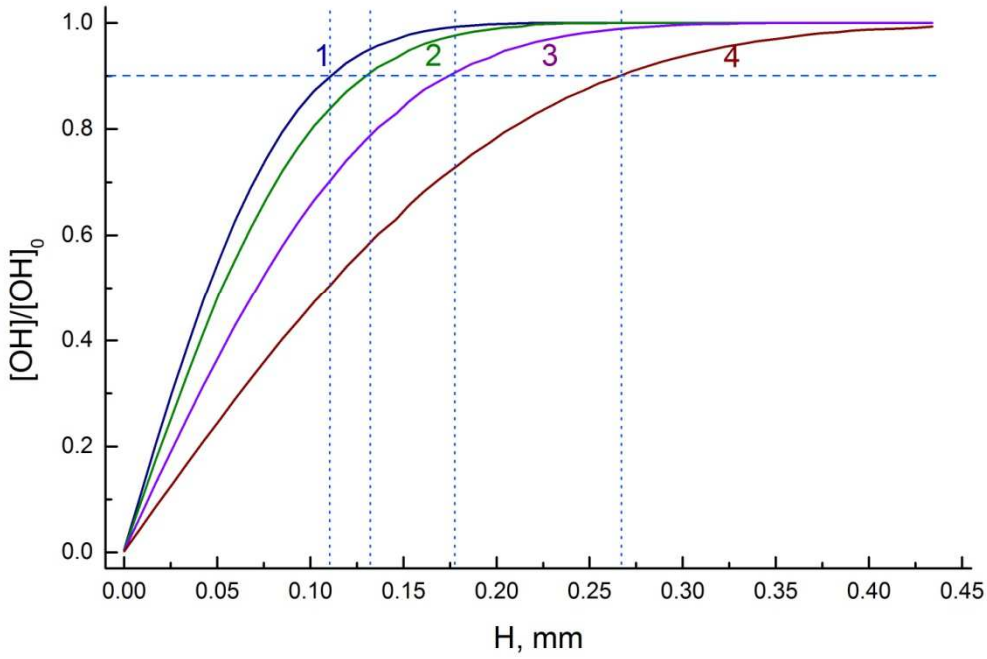

Figure 10. Relative concentration of OH groups at a depth *H* from a surface of a flat KU-1 glass plate after annealing for 100 hours. Temperature of annealing: *1* – 825°C; *2* – 850°C; *3* – 900°C; *4* – 980°C. Dotted vertical lines show the depth of the dehydroxylated layer.

Let us consider the depth of the dehydroxylated layer H for $\frac{[OH]}{[OH]_0} = 0.9$. This value depends on both the temperature and duration of the annealing, T_0 and t_0, respectively. Figure 11 shows the increase of the depth H of the dehydroxylated layer for four annealing temperatures. Summarizing the above, we can write the dependence $H(T_0, t_0)$, for type III silica glass, annealed at temperatures ranging from 800^0C to 980^0C by the empirical expression:

$$H = (10^{-4} \times T_0 - 0.1)\sqrt{t_0}\,, \tag{8}$$

where the depth H is measured in mm, the temperature of annealing T_0 in K, and the annealing duration t_0 in hours.

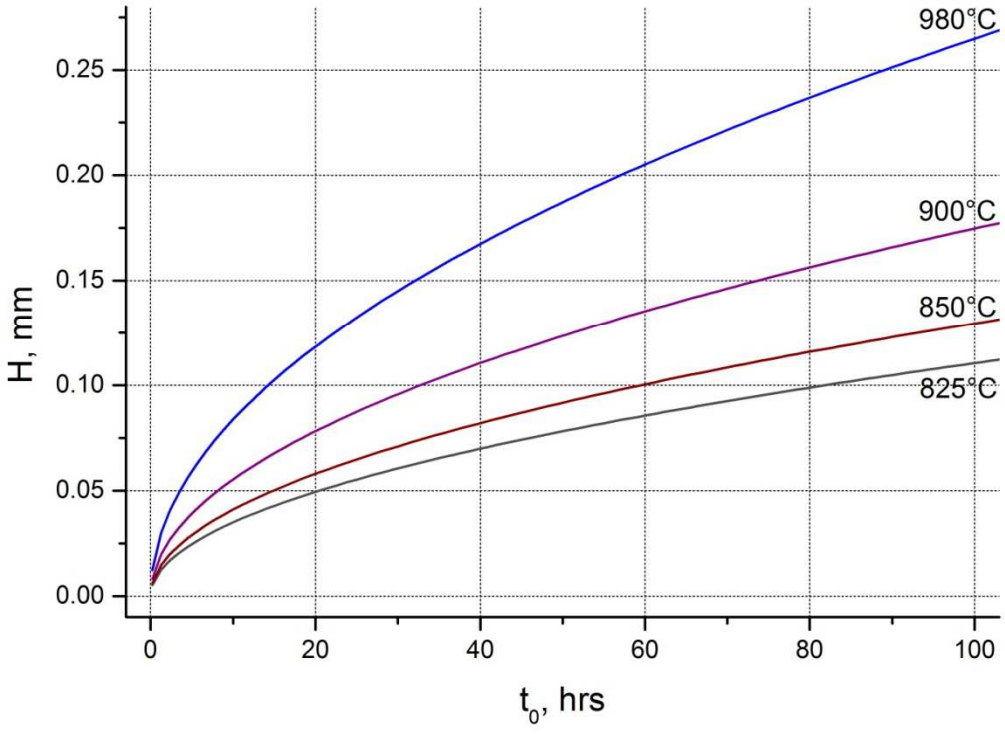

Figure 11. Kinetics of the growth of the dehydroxylated surface layer depth during annealing at different temperatures.

The volume of glass near the surface tries to become smaller after dehydroxylation. However the Si and O atoms are embedded in the bulk structure, keeping its rigidity. The volume of the glass sample remains the same. Egress of the hydroxyl groups leaves so-called dangling bonds, which can couple to form stretched bonds between silicon and oxygen atoms. The near-surface layer becomes peppered with randomly-distributed tensile stresses. The total sum of these stresses drops to zero at the depth *H*. To the first approximation, we can assume that the average value of these stresses σ_{dihyd} does not depend on the depth *H* and is equal to

$$\sigma_{\text{dihyd}} = \frac{E\varepsilon}{2} \cdot e^{\frac{-t_0}{\tau}}, \qquad (9)$$

where *E* is Young's modulus of the silica glass, ε is the strain of the silica glass after dehydroxylation (which can be set to $\varepsilon \approx 10^{-3}$ for glasses of type III), and τ is the characteristic time of silica glass relaxation. The second term in (9) describes the relaxation of the structure of silica glass that occurs simultaneously with the dehydroxylation of the glass surface.

The surface stresses might lead to the formation of surface cracks. The surface of the mechanically-polished glass always contains linear defects, which can act as the nucleus of surface cracks. For crack-growth to initiate, the nearby internal stress should exceed some critical value σ_{crit}, which depends on the length of the defect, i.e., the depth of the dehydroxylated layer *H* [42]:

$$\sigma_{crit} = \frac{K_{crit}}{\sqrt{\pi H}} \ . \qquad (10)$$

The parameter K_{crit} is a critical intensity factor (for silica glass, this value can be tentatively taken as a constant equal to 5×10^5 Pa $\cdot \sqrt{\text{m}}$ [43,44].)

As the depth of the dehydroxylated layer increases during annealing, σ_{crit} diminishes and; if it becomes smaller than the level of internal stress, a crack appears on the glass surface. In this way, the annealing of type III silica glass activates two parallel processes at the glass surface. The first

is the formation of a stressed dehydroxylated layer, triggering the growth of surface cracks. The second is structural relaxation accompanied by the relaxation of internal stress. Considering both processes, we calculated the change in $\sigma_{\text{dihyd}}(t)$ and $\sigma_{\text{crit}}(t)$ with time for four annealing temperatures. Figure 12 presents the calculation of the difference between internal and critical stresses

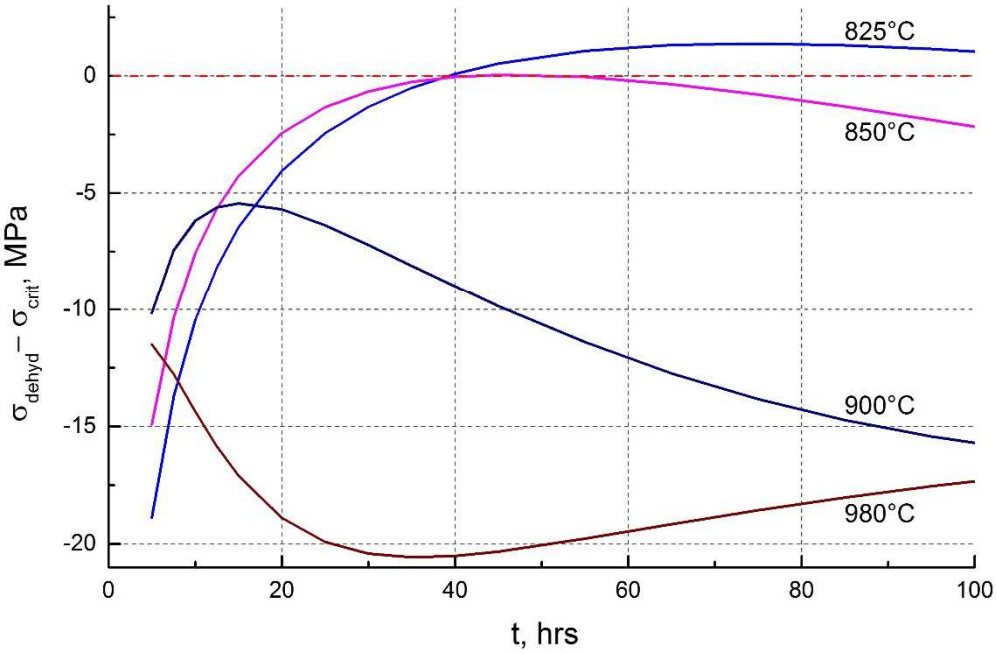

Figure 12. Changes of the difference between internal and critical stresses $[\sigma_{dehyd} - \sigma_{crit}]$ in the near-surface layer during annealing at different temperatures.

in the near-surface layer in type III silica glass in the course of annealing at the fixed temperatures 825, 850, 900, and 980^{0}C. The value of internal stress corresponding to the annealing temperature 825^{0}C exceeds the critical threshold ($i.e.[\sigma_{dehyd} - \sigma_{crit}] > 0$) after 40 hours of annealing. Longer annealing will activate the formation of surface cracks. However, internal stress is always lower than the critical value $\sigma_{\text{dihyd}} < \sigma_{\text{crit}}$ during annealing at $T \geq 850^0$C; formation of cracks at these annealing temperatures is unlikely.

This conclusion is supported by studies of the surface of silica glass samples that have been annealed for 600 hours, which were presented previously [40]. The surface of type III samples annealed at a temperature below 850^0C, is covered by a well-developed pattern of cracks. The surface of KU-1 samples annealed at higher temperatures contain only single defects. We can assume that these defects were developed from seeds (local stressed zones) remaining from the preceding mechanical treatment. The formation of cracks caused by dehydroxylation of the surface does not occur in OH-free silica glasses. A sample of a similar size made from silica glass KS4V (with a concentration of the OH group smaller than 1ppm) was also annealed for 600 hours at 825^0C. However, no crack-growth was observed on its surface.

The influence of the surface cracks on the Q factor can be sufficiently large. The phenomenon of surface losses is usually linked with the scattering of surface acoustic waves (Rayleigh waves) [45]. Any surface irregularities increase such scattering, and, hence, increase the energy dissipation. This effect was observed in many materials[46–48] , including the influence of surface micro-cracks on the Q factor of silica glass fibres[49]. B. Lunin also observed an increase of losses when measuring the oscillation of cylinders from silica glass after one early annealing. The Q-factor in those experiments was significantly improved after re-grinding and re-polishing the silica surface[50].

7. Optimal regime of annealing of type III silica glass.

General discussion and conclusion

Let us summarize the results presented above. The internal stress formed in a silica-glass object during its fabrication is one of the main factors limiting internal friction. Such objects can be used as high-Q resonators only if the level of residual stress is ~10^4 Pa (≈ 0.1kg/cm^2) or smaller.

Isothermal annealing is the main means of stress reduction. Heating a silica-glass sample to temperatures above ~800^0C causes a process of rearrangement of the atomic network towards a state of equilibrium. Continuance of such rearrangement (for the duration of the annealing)

depends on temperature (Table 1). Cooling of the heated sample again generates stresses in the atomic structure. This process depends on the temperature of the annealing and the cooling rate. Note that a relatively slow cooling rate does not ensure minimal internal friction by itself. The degree to which the internal stress accumulates is very sensitive to the annealing temperature. Changing the temperature triggers new modification of the atomic structure. The duration of the cooling-down period to the critical temperature ~750°C is likely too short for completing this modification. The atomic network remains in-between two equilibrium states. The non-equilibrium atomic chains were described above as distorted structural elements. In addition, the atomic chains effectively freeze in stressed conditions due to the temperature gradient occurring during cooling. Both these factors contribute to the rise of internal friction in the silica-glass sample. We evaluated the contribution of these factors depending on the temperature of annealing and the rate of cooling. The low annealing temperature (which, certainly, requires a longer annealing time) reduces the influence of stress and distortion on the level of mechanical losses. Test samples 0.1m in diameter, annealed at 800°C, will suffer a sufficiently small increase in internal friction irrespective of the rate of cooling. However, we still cannot recommend 800°C for annealing articles made from type III silica glass. The heating of silica-glass samples extracts hydroxyl groups from the near-surface layer. Dehydroxylation of the glass provokes a rise in the stress near the surface of the glass and hence the formation of cracks. This process is likely to occur for temperatures ≤825°C while the growth of cracks at larger annealing temperatures ($T \geq$ 850°C) is less likely.

Summarizing all these factors, we recommend that articles fabricated from type III silica glass should be annealed at temperatures 850-900^{0}C. The duration of the annealing depends non-linearly on the temperature. It ranges from ~ 240 hours for 850^{0}C to ~ 50 hours for 900^{0}C. The rate of cooling to 750^{0}C should be calculated in relation to the size of the glass article and an acceptable value for the residual stress. The following cooling from 750^{0}C to room temperature can be performed in the oven without additional control over the cooling rate. This regime ensures low

inner stress of the siloxane bonds, the small distortion of the equilibrium structure during cooling and the zero rise of new surface cracks.

The efficiency of this approach is confirmed by the measurements of mechanical loss in test samples annealed at different temperatures. Let us return to Figure 2. The *Q* factor is measured at frequencies near 30-40 kHz in the temperature range 50–250°C, which is important for practical applications. The sample annealed at 900°C shows a *Q* factor larger than a similar sample annealed at 980°C and much larger than a non-annealed test sample. The type IV glass samples, measured as delivered, manifested larger losses (smaller *Q* factor) in comparison with the carefully annealed articles made from the type III glass. These data confirm that silica glass with large OH content can be used as a relatively cheap material for fabrication of mechanical resonators with a *Q* factor approaching 10^8.

Note that spectroscopic measurements are used to control the heat treatment, not only of pure silica glass samples, but also of multicomponent glasses[51,52]. It is known that annealing changes many physical properties of silicate glasses[53,54]. We propose that our approach may enhance methods for the experimental study of such properties in annealed glass samples.

Acknowledgments

We are grateful to the Royal Society in the UK and the Russian Foundation for Basic Research which have allowed the authors to collaborate within the International Exchanges Scheme - 2016 under Royal Society Cost Share Grant IE160125 and RFBR Grant 16-52-10069. We wish to thank all our colleagues from faculties of Physics and Chemistry at M.V. Lomonosov Moscow State University and the Institute for Gravitational Research at University of Glasgow for help and support. We are also thankful to our colleagues in the GEO600, LIGO Scientific Collaboration, Virgo and KAGRA for their interest in this work. We would also like to show our gratitude to Dr I. Martin and Dr V. Macaulay from University of Glasgow for proofreading of the paper draft.

References

1. Rozelle DM. The hemispherical resonator gyro: From wineglass to the planets. In: Advances in the Astronautical Sciences. 2009. p. 1157–78.
2. Jeanroy A, Bouvet A, Remillieux G. HRG and marine applications. Gyroscopy Navig. 2014;5(2):67–74.
3. Ahamed MJ, Senkal D, Shkel AM. Effect of annealing on mechanical quality factor of fused quartz hemispherical resonator. In: 1st IEEE International Symposium on Inertial Sensors and Systems, ISISS 2014 - Proceedings. 2014.
4. Cho J, Yan J, Gregory JA, Eberhart H, Peterson RL, Najafi K. High-Q fused silica birdbath and hemispherical 3-D resonators made by blow torch molding. In: Proceedings of the IEEE International Conference on Micro Electro Mechanical Systems (MEMS). 2013. p. 177–80.
5. Aasi J. et al. Advanced LIGO. Class Quantum Gravity. 2015;32(7):074001.
6. Aston SM et al. Update on quadruple suspension design for Advanced LIGO. Class Quantum Gravity. 2012;29(23):235004.
7. Gillespie A, Raab F. Thermally excited vibrations of the mirrors of laser interferometer gravitational-wave detectors. Phys Rev D. 1995;52(2):577–85.
8. Bruckner R. Properties and structure of vitreous silica. I. J Non Cryst Solids. 1970;5(2):123–75.
9. Hetherington G, Jack KH, Ramsay MW. The high-temperature electrolysis of vitreous silica. Phys Chem Glas. 1965;6(1):6–15.
10. Hyde JF. Method of making a transparent article of silica. US Patent; 2,272,342, 1942.
11. Seward TP. Silica Glass Processing [Internet]. 2015. Available from: http://www.lehigh.edu/imi/teched/GlassProcess/Lectures/Lecture18_Seward_SilicaGlassProcessing2.pdf
12. Lunin BS, Torbin SN. Internal friction in quartz glass at moderate temperature. Moscow Univ Chem Bull. 2000;55(2):30–2.
13. Quartz Glass for Optics [Internet]. Available from:

http://www.tydexoptics.com/materials1/for_mirrors/fused_silica/

14. Suprasil® and Infrasil® – Material Grades for the Infrared Spectrum [Internet]. Available from: https://www.heraeus.com/media/media/hqs/doc_hqs/products_and_solutions_8/optics/Suprasil_and_Infrasil__Material_Grades_for_the_Infrared_Spectrum_EN.pdf

15. Crooks DRM, Sneddon P, Cagnoli G, Hough J, Rowan S, Fejer MM, et al. Excess mechanical loss associated with dielectric mirror coatings on test masses in interferometric gravitational wave detectors. Class Quantum Gravity. 2002;

16. Rowan S, Twyford SM, Hough J, Gwo DH, Route R. Mechanical losses associated with the technique of hydroxide-catalysis bonding of fused silica. Phys Lett Sect A Gen At Solid State Phys. 1998;

17. Mitrofanov VP, Chao S, Pan H-W, Kuo L-C, Cole G, Degallaix J, et al. Technology for the next gravitational wave detectors. Sci China Physics, Mech Astron. 2015;

18. Rowan S, Cagnoli G, Sneddon P, Hough J, Route R, Gustafson EK, et al. Investigation of mechanical loss factors of some candidate materials for the test masses of gravitational wave detectors. Phys Lett Sect A Gen At Solid State Phys. 2000;

19. Sanin VI, Skripnikov VA, Krenev YL. Effect of deformation on the low-temperature ultrasonic absorption in vitreous silica. Sov J Glas Phys Chem. 1990;15(3):297–301.

20. Strakna RE, Clark AE, Bradley DL, Slie WM. Effect of Fast-Neutron Irradiation on the Pressure and Temperature Dependence of the Elastic Moduli of SiO_2 Glass. J Appl Phys. 1963;34(5):1439–43.

21. Galeener FL. Planar rings in vitreous silica. J Non Cryst Solids. 1982;49(1–3):53–62.

22. Rino JP, Ebbsjö I, Kalia RK, Nakano A, Vashishta P. Structure of rings in vitreous SiO_2. Phys Rev B. 1993;47(6):3053–62.

23. Jin W, Kalia RK, Vashishta P, Rino JP. Structural transformation in densified silica glass: A molecular-dynamics study. Phys Rev B [Internet]. 1994 Jul 1;50(1):118–31. Available from: https://link.aps.org/doi/10.1103/PhysRevB.50.118

24. Le Roux S, Jund P. Ring statistics analysis of topological networks: New approach and application to amorphous $GeS_2$and SiO_2systems. Comput Mater Sci. 2010;

25. Charpentier T, Kroll P, Mauri F. First-principles nuclear magnetic resonance structural analysis of vitreous silica. J Phys Chem C. 2009;

26. Edén M. NMR studies of oxide-based glasses. Annual Reports on the Progress of Chemistry - Section C. 2012.

27. Martinet C, Kassir-Bodon A, Deschamps T, Cornet A, Le Floch S, Martinez V, et al. Permanently densified SiO_2 glasses: A structural approach. J Phys Condens Matter. 2015;

28. Charpentier T, Menziani MC, Pedone A. Computational simulations of solid state NMR spectra: A new era in structure determination of oxide glasses. RSC Advances. 2013.

29. Ebrahem F, Bamer F, Markert B. The influence of the network topology on the deformation and fracture behaviour of silica glass: A molecular dynamics study. Comput Mater Sci. 2018;

30. Koziatek P, Barrat JL, Rodney D. Short- and medium-range orders in as-quenched and deformed SiO2glasses: An atomistic study. J Non Cryst Solids. 2015;

31. Sundararaman S, Ching WY, Huang L. Mechanical properties of silica glass predicted by a pair-wise potential in molecular dynamics simulations. J Non Cryst Solids. 2016;

32. Pasquarello A, Car R. Identification of Raman Defect Lines as Signatures of Ring Structures in Vitreous Silica. Phys Rev Lett [Internet]. 1998 Jun 8;80(23):5145–7. Available from: https://link.aps.org/doi/10.1103/PhysRevLett.80.5145

33. Agarwal A, Davis KM, Tomozawa M. A simple IR spectroscopic method for determining fictive temperature of silica glasses. J Non Cryst Solids. 1995;185(1–2):191–8.

34. Zverev VA, Krivopustova EV, Tochilina TV. Optical Materials. [Internet]. St. Petersburg: ITMO University; 2013. 248 p. Available from: http://books.ifmo.ru/file/pdf/1358.pdf

35. Primak W. The annealing of vitreous silica. PhysChemGlass. 1983;24(1):8–17.

36. Nowick AS, Berry BS. Anelastic relaxation in crystalline solids. New York: Academic Press; 1972. 694 p.

37. Manohar PA, Ferry M, Chandra T. Five Decades of the Zener Equation. ISIJ Int [Internet]. 1998;38(9):913–24. Available from: http://joi.jlc.jst.go.jp/JST.Journalarchive/isijinternational1989/38.913?from=CrossRef

38. Moczo P, Kristek J, Franek P. Lecture Notes on Rheological Models [Internet]. Bratislava; 2006.

Available from:
http://www.fyzikazeme.sk/mainpage/stud_mat/Moczo_Kristek_Franek_Rheological_Models.pdf

39. Anderson OL, Bommel HE. Ultrasonic Absorption in Fused Silica at Low Temperatures and High Frequencies. J Am Ceram Soc [Internet]. 1955 Apr;38(4):125–31. Available from: http://doi.wiley.com/10.1111/j.1151-2916.1955.tb14914.x

40. Lunin BS, Kharlanov AN, Kozlov SE. Dehydroxylation and formation of KU-1 silica glass surface defects during annealing. Moscow Univ Chem Bull. 2010;65(1):34–7.

41. Crank J. The mathematics of diffusion [Internet]. Second. Oxford: Clarendon Press; 1979. 414 p. Available from: http://www.ees.nmt.edu/outside/courses/hyd510/PDFs/SupplementaryReadings/Crank_1975_Diffusion.pdf

42. Patron VZ. Mekhanika razrusheniya: ot teorii k praktike (Fracture mechanics: from theory to practice). Reprint of. Moscow: Editorial URSS; 2016. 240 p.

43. Hibino Y, Sakaguchi S, Tajima Y. Crack growth in vitreous silica under dynamic loading. J Mater Sci Lett. 1983;2(8):388–392.

44. Hibino Y, Sakaguchi S, Tajima Y. Crack growth in silica glass under dynamic loading. J Am Ceram Soc. 1984;67(1):64–8.

45. Hess P. Surface Acoustic Waves in Materials Science. Phys Today [Internet]. 2002 Mar;55(3):42–7. Available from: http://physicstoday.scitation.org/doi/10.1063/1.1472393

46. Nawrodt R, Schwarz C, Kroker S, Martin IW, Bassiri R, Brückner F, et al. Investigation of mechanical losses of thin silicon flexures at low temperatures. Class Quantum Gravity. 2013;30(11):115008 (12pp).

47. Carr DW, Evoy S, Sekaric L, Craighead HG, Parpia JM. Measurement of mechanical resonance and losses in nanometer scale silicon wires. Appl Phys Lett. 1999;75(7):920–2.

48. Wang Y, Henry J a, Zehnder a T, Hines M a. Surface Chemical Control of Mechanical Energy Losses in Micromachined Silicon Structures. J Phys Chem B. 2003;107(51):14270–14277.

49. Gretarsson AM. Effect of optical coating and surface treatments on mechanical loss in fused silica. In: AIP Conference Proceedings [Internet]. AIP; 2000. p. 306–12. Available from:

http://aip.scitation.org/doi/abs/10.1063/1.1291872

50. Lunin BS, Torbin SN. Formation of quartz glass surface defects under thermal treatment conditions. Moscow Univ Chem Bull. 2005;60(6):16–9.

51. Vaills Y, Luspin Y, Hauret G. Annealing effects in SiO2–Na2O glasses investigated by Brillouin scattering. J Non Cryst Solids [Internet]. 2001;286(3):224–34. Available from: https://www.sciencedirect.com/science/article/pii/S0022309301005233

52. Khalil EMA, Aouf M. Effect of heat treatment on the infrared absorption spectra of strontium-sodium-borosilicate glass. IJEMS [Internet]. 1997;4:155–62. Available from: http://nopr.niscair.res.in/bitstream/123456789/29732/1/IJEMS 4%284%29 155-162.pdf

53. Surovtsev N V., Wiedersich J, Batalov a. E, Novikov VN, Ramos M a., Rössler E. Inelastic light scattering in B2O3 glasses with different thermal histories. J Chem Phys. 2000;113:5891.

54. Munishwar SR, Pawar PP, Gedam RS. Influence of electron-hole recombination on optical properties of boro-silicate glasses containing CdS quantum dots. J Lumin. 2017;